

Supplementary Information: Tropical tree drought sensitivity is jointly shaped by drought characteristics, species adaptations, and individual microenvironments

Contents

Climate data and correlations	2
Data cleaning additional methods	4
Growth timeseries and anomalies	5
Drought year growth of species and individuals	7
Variables and their distributions	9
Raw sensitivity and residuals with predictors	12
Conditional dependencies	15
Alternate models using Topographic Position Index	18

References	18
-------------------	-----------

Authors

Krishna Anujan^{1,2*} ORCID: 0000-0003-3604-5895
Sean McMahon^{2,3} ORCID: 0000-0001-8302-6908
Sarayudh Bunyavejchewin⁴ ORCID: 0000-0002-1976-5041
Stuart J. Davies³ ORCID: 0000-0002-8596-7522
Helene C. Muller-Landau³ ORCID : 0000-0002-3526-9021
Nantachai Pongpattananurak⁵ ORCID: 0000-0001-8687-6182
Kristina Anderson-Teixeira^{1,3} ORCID: 0000-0001-8461-9713

Climate data and correlations

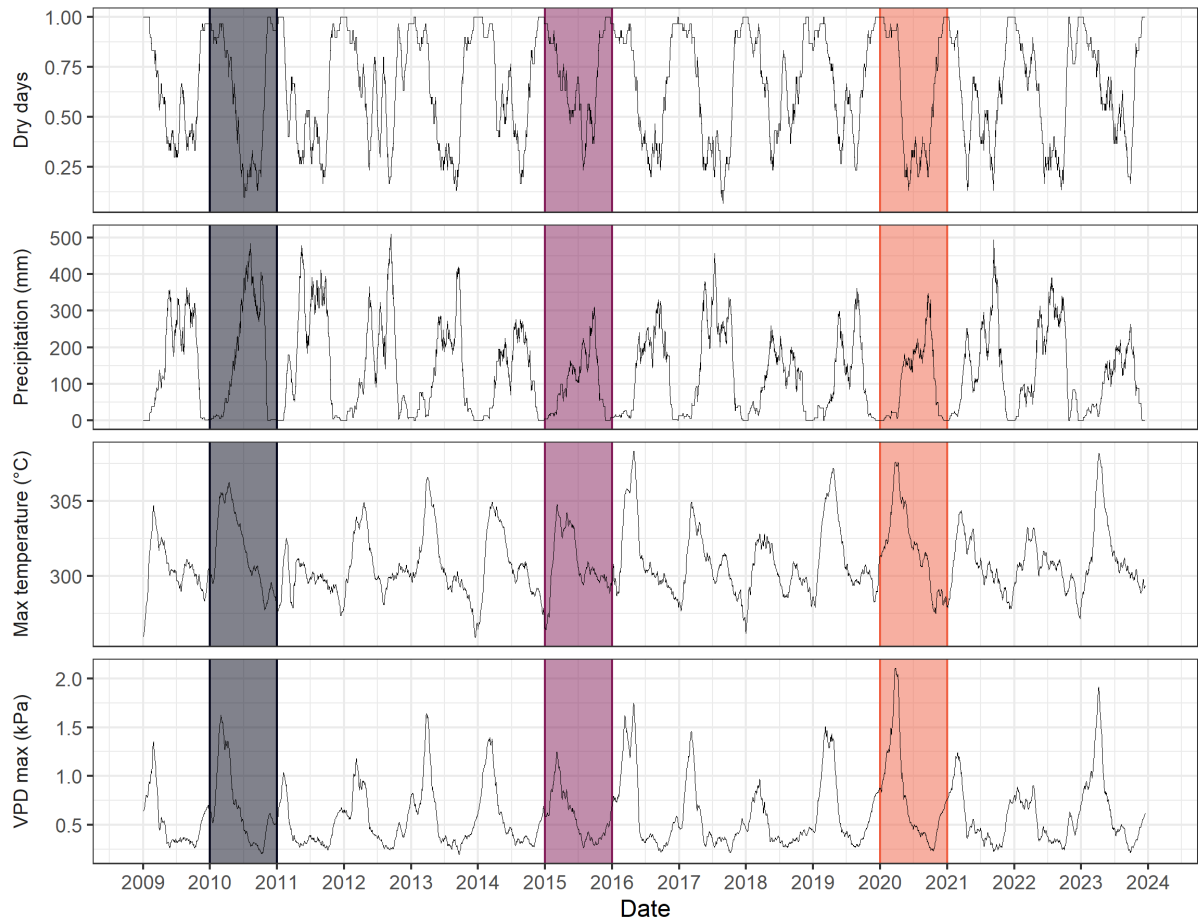


Figure S1: Raw climate data timeseries from 2009 to 2023 from ERA5Land and CHIRPS. Measurements represent daily rolling means over a 30-day time window for precipitation, max temperature and VPD and rolling sum for number of dry days.

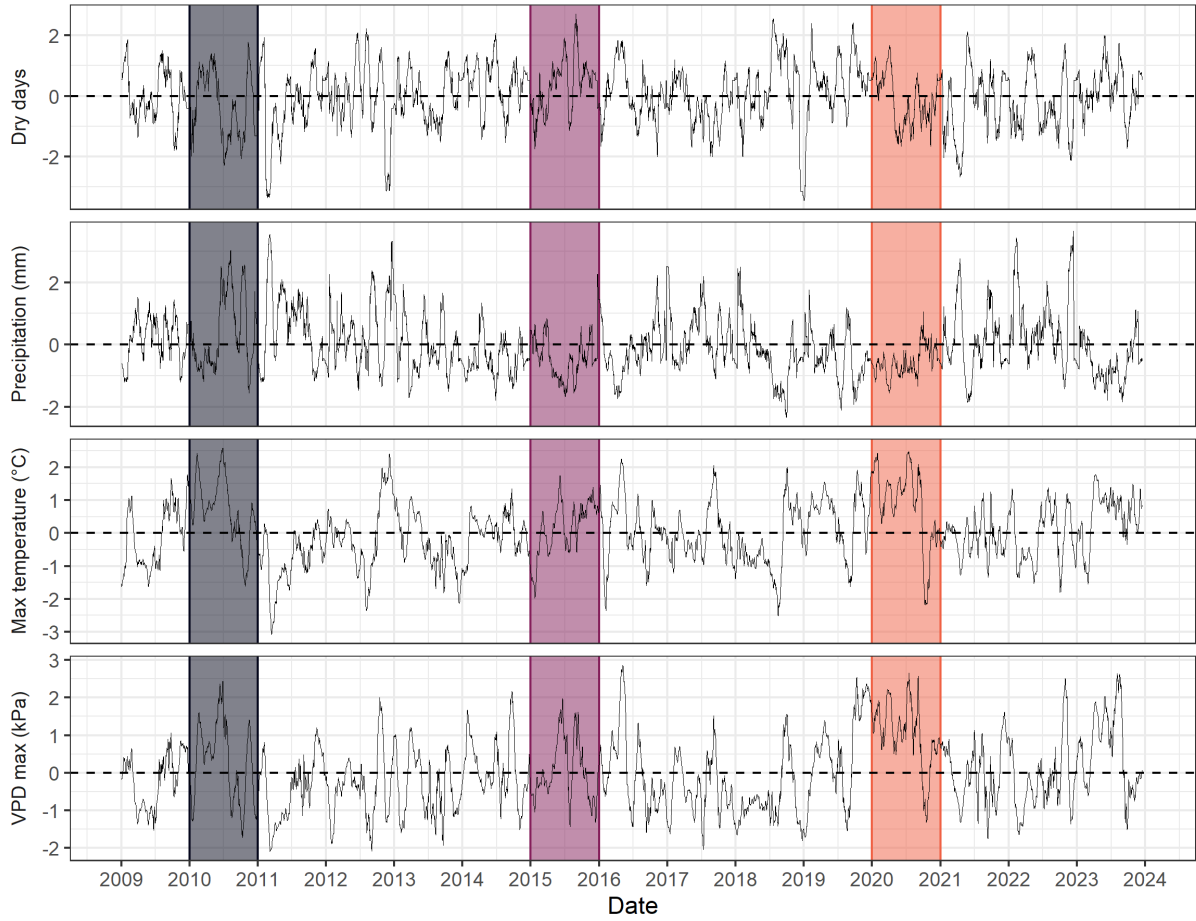


Figure S2: Climate anomalies for all variables from 2009 to 2020. Values represent number of standard deviations from the long-term mean for daily rolling mean values.

Data cleaning additional methods

For raw measurements of dendrometer band window size, we conducted QAQC steps as follows: 1. Removed potentially misidentified individuals. We removed individuals with conflicting metadata on tag or location across censuses. We did not remove individuals with conflicting species identification because these are often updated during the ForestGEO censuses. Therefore, we used the latest version of species identification for each tag shared by the PIs of the HKK plot. 2. Removed potential misidentified bands. Each new dendroband installed on a tree is numbered sequentially starting from 1. We removed any measurements made on bands old bands after a new band series had begun. 3. Removing measurements that appeared likely to be data entry errors. We identified misplaced decimals by checking if the ratio between adjacent window size measurements were closer to 1 or 10 or 100. We removed measurements that had ratios closer to 10 or 100 than 1, assuming that these were likely misplaced decimals.

After calculating DBH from window size measurements and calculating annualised growth increments, we conducted further QAQC on these increments to create the final dataset: 1. We excluded large measurement outliers, defined as > 3 standard deviations from the mean increment across all observations. 2. We excluded trees with negative increments or increments close to zero over the whole timeseries of observations. These low growing trees may be indicative of stress or mortality, and likely to bias analysis of interannual growth variation. 3. We used concurrent tape measurements on dendrobanded trees to flag likely errors. We calculated annualised increments from annual tape measurements made on each dendrobanded tree at each census, using similar methods as described for dendrometer bands. For each tree and year, we calculated the degree of deviation of these measurements from each other as the Euclidean distance from the 1:1 line. We found that 90% of the increments were within 5 mm of of deviation, which we retained as a high confidence dataset. We excluded the remaining 10% from the analysis, although we were unable to ascertain whether the discrepancy was because of errors in tape or dendroband measurements.

Growth timeseries and anomalies

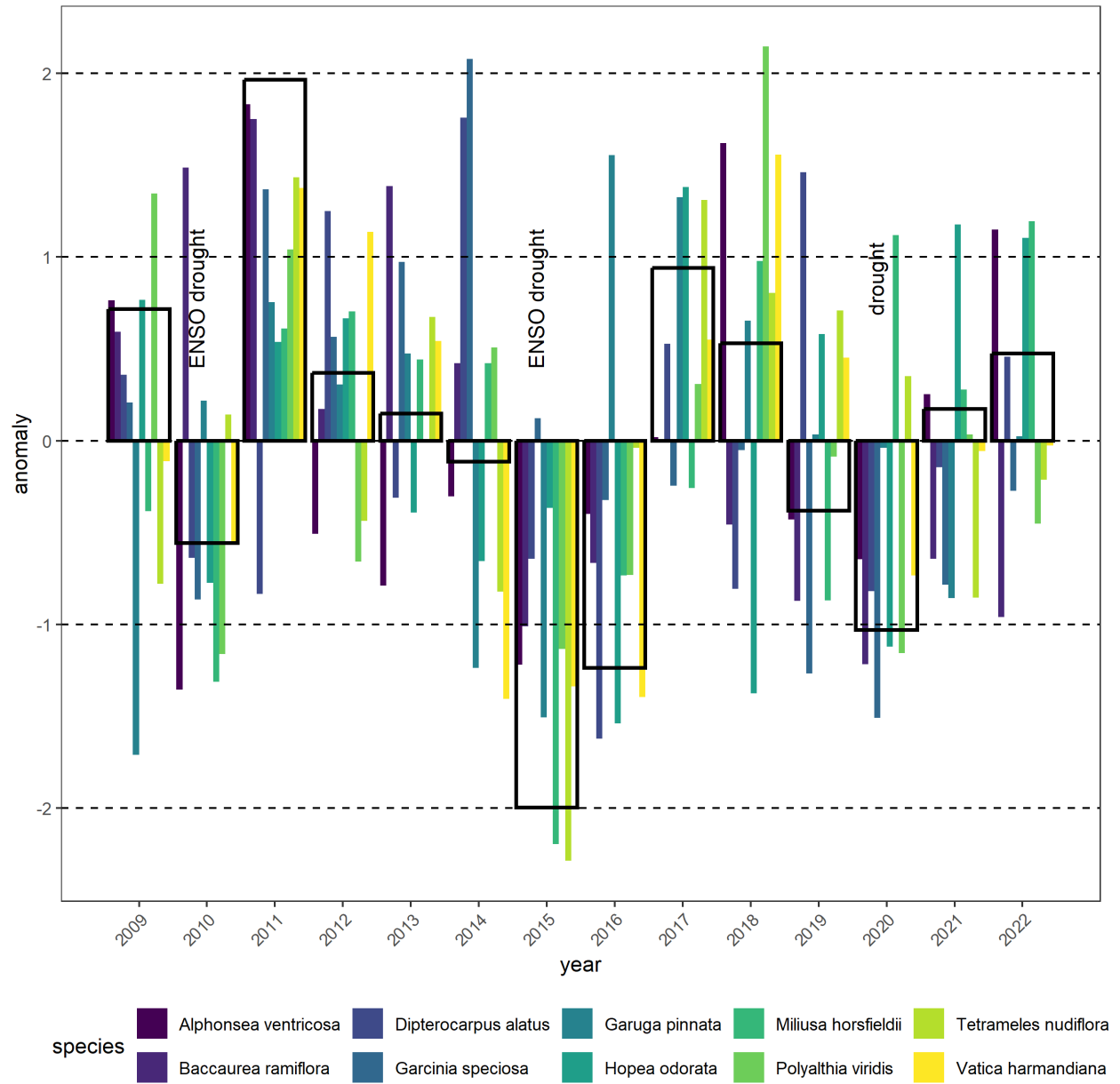


Figure S3: Growth anomalies across the timeseries. Growth anomalies for each year calculated as the number of standard deviations in growth each year from mean growth across all years and summarised for plot and species.

Drought year growth of species and individuals

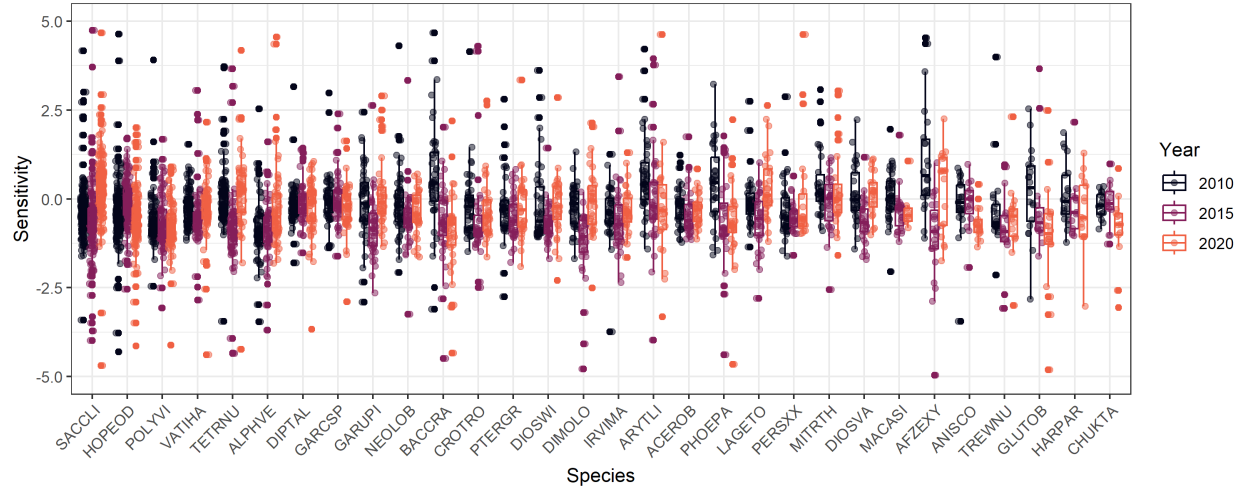


Figure S4: Species sensitivities in drought years 2010 and 2015. Boxplots represent 25th, 50th (median) and 75th percentile of sensitivity for each species in each year and whiskers represent 95% CIs. All individual sensitivities represented by jittered points.

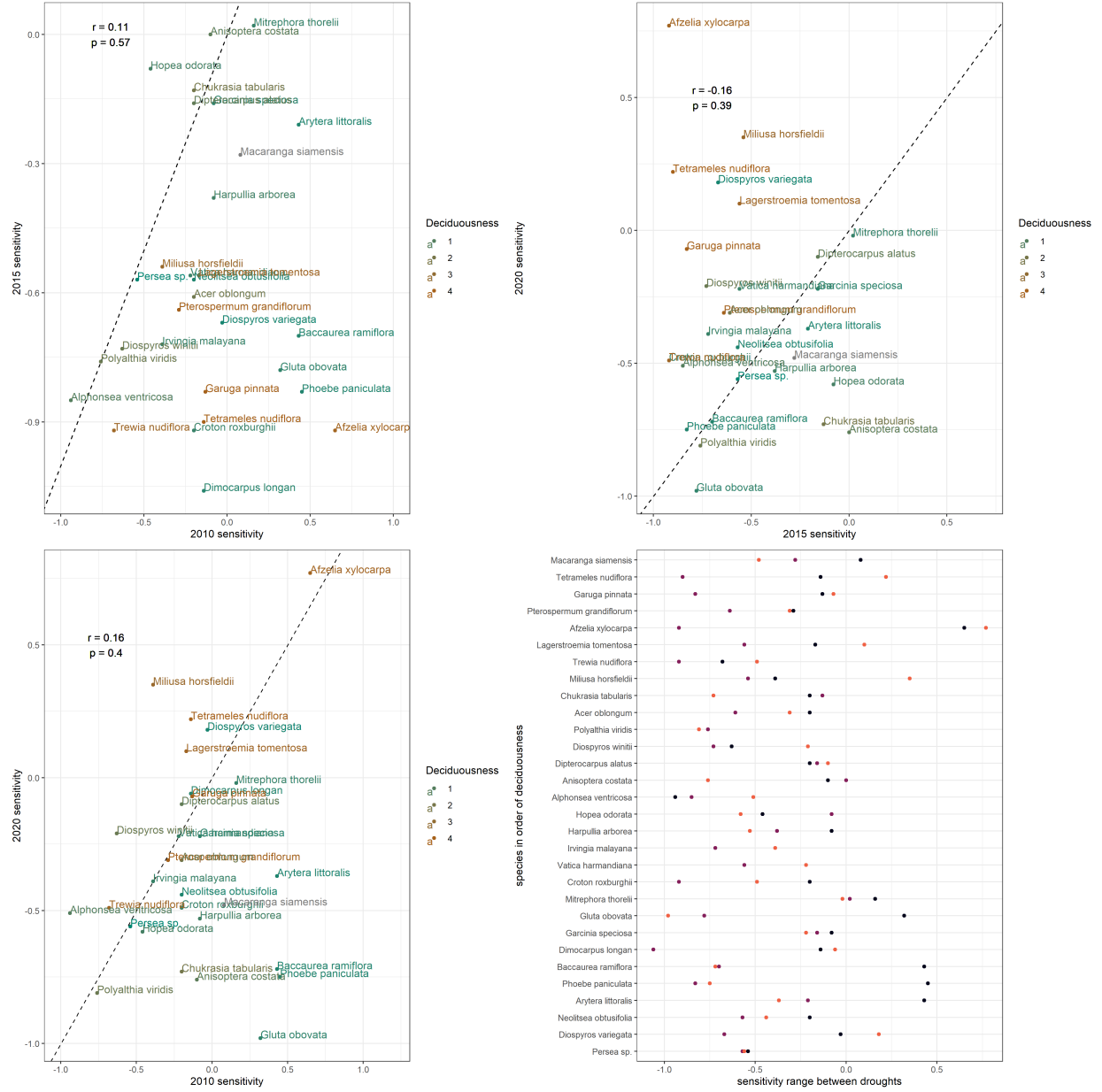


Figure S5: Correlations of species sensitivities across the two years. Panel a shows correlation of species median sensitivities in the two years and Pearson's correlation coefficient. Colour gradient represents deciduousness scale and dotted line is the 1:1 line. Panel b shows difference in magnitude of species median sensitivities among the two years

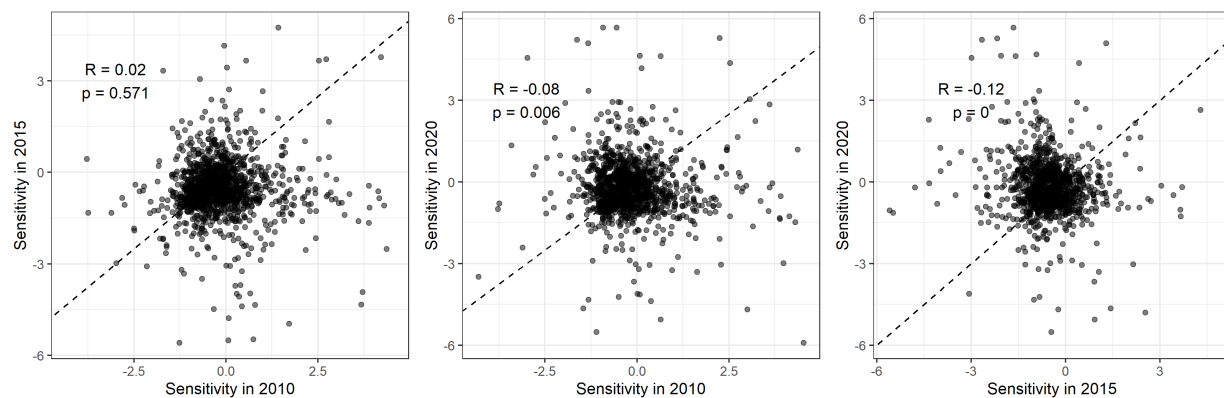


Figure S6: Correlation of individual sensitivities across the two years along with Pearson’s correlation coefficient and the 1:1 line.

Variables and their distributions

Map of trees

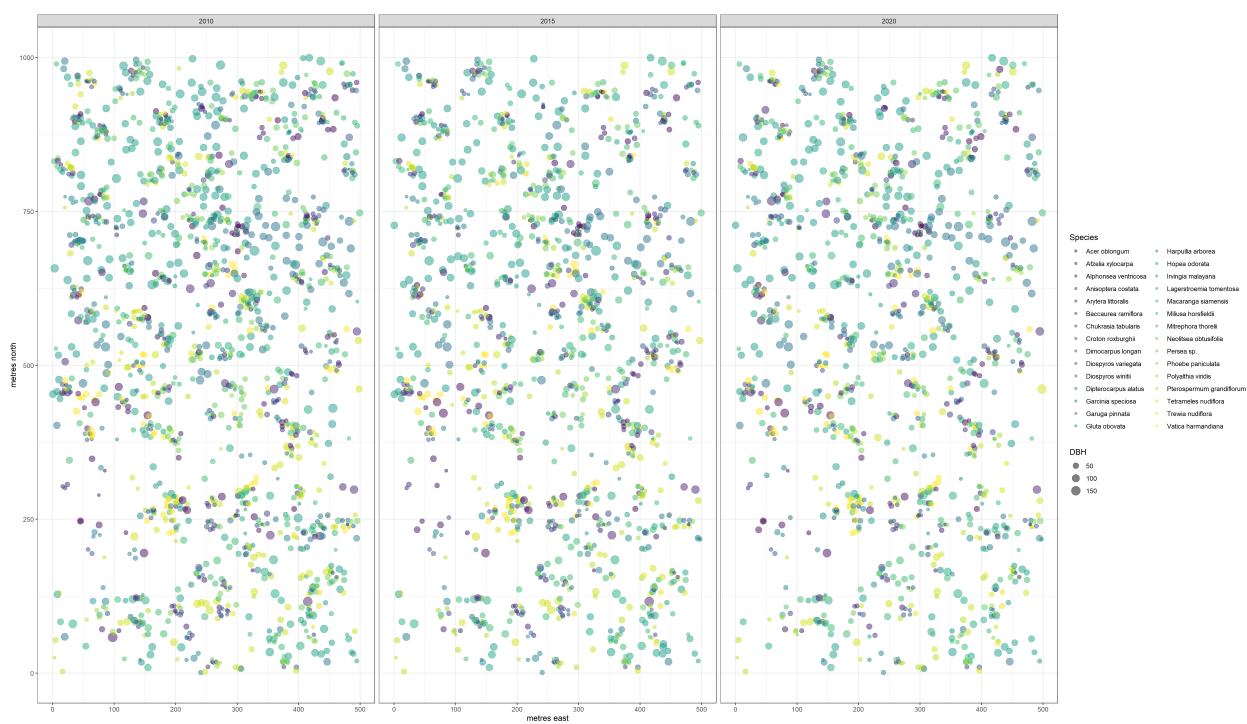


Figure S7: Map of trees with dendrobands in HKK, included in analyses in the 2010 and 2015 datasets

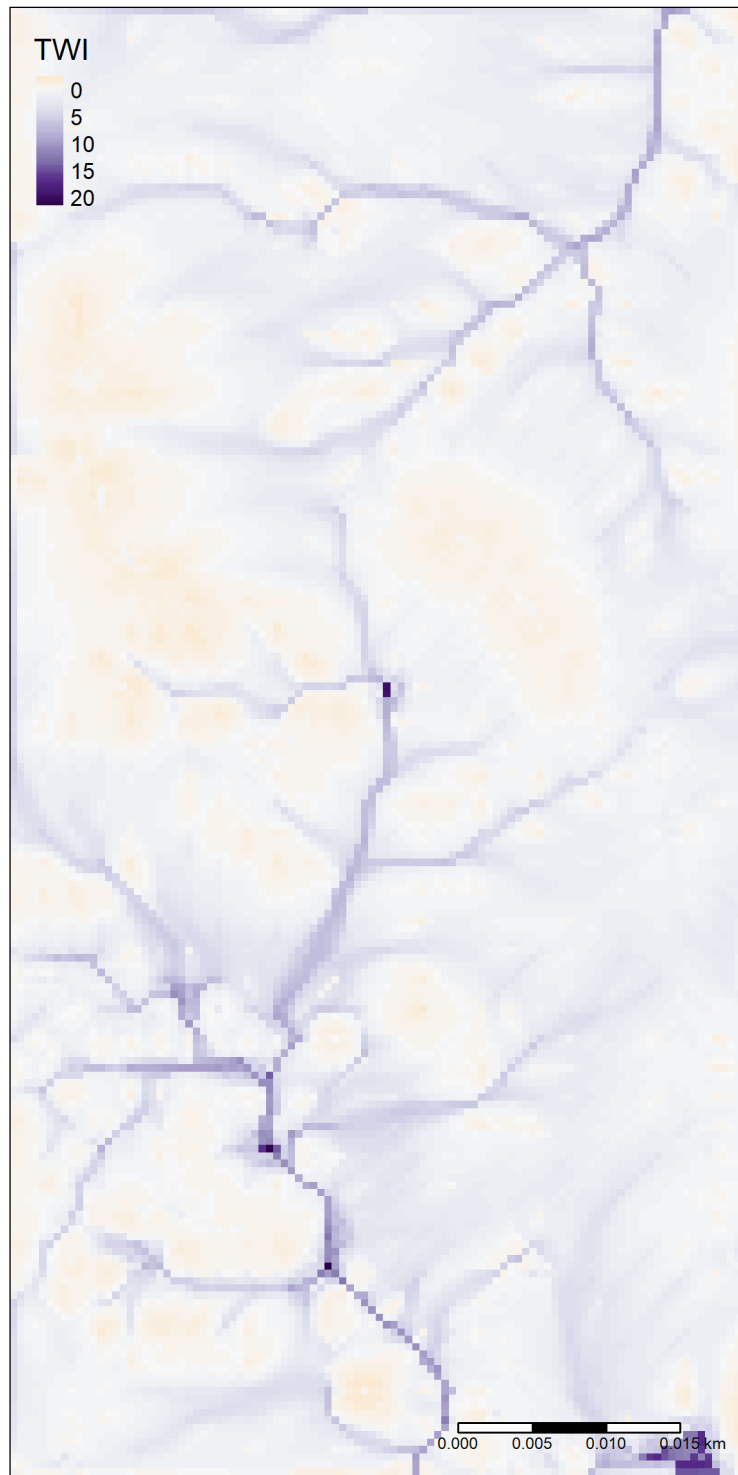


Figure S8: Calculated Topographic Wetness Index (TWI) values for the HKK plot

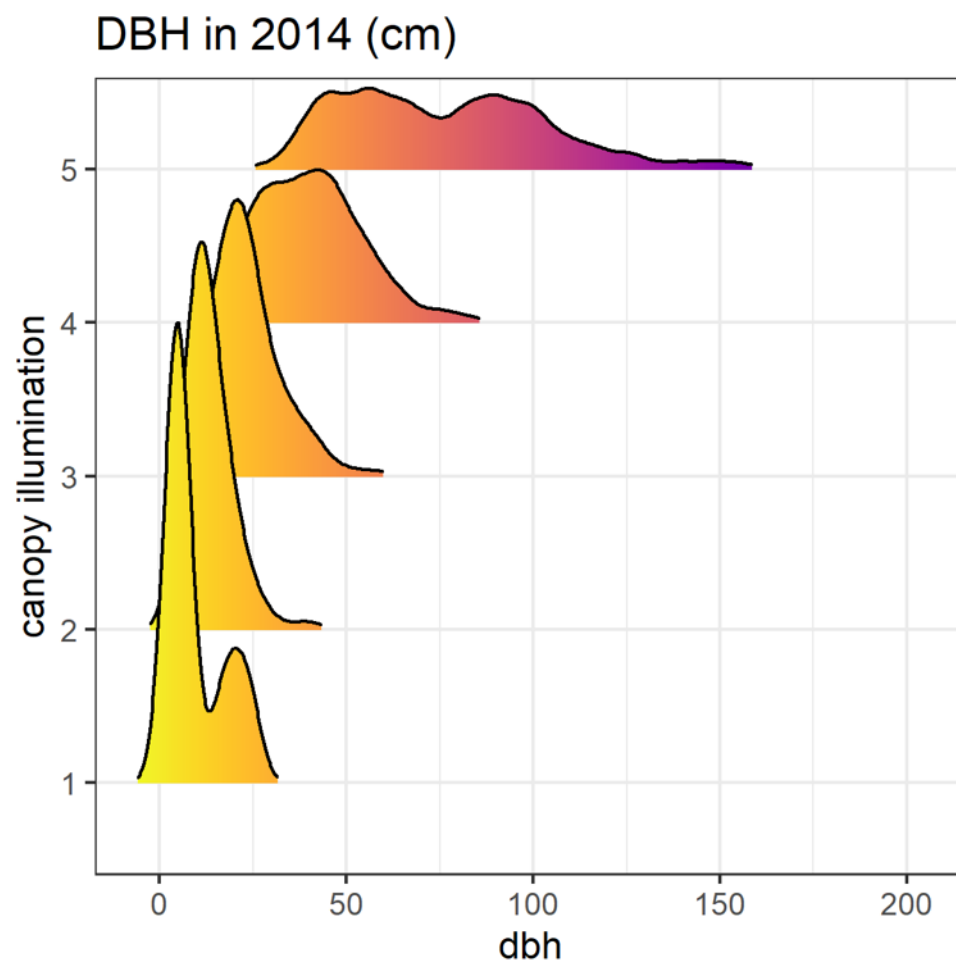


Figure S9: Distribution of DBH with Crown Illumination Index (CII) in 2014.

Raw sensitivity and residuals with predictors

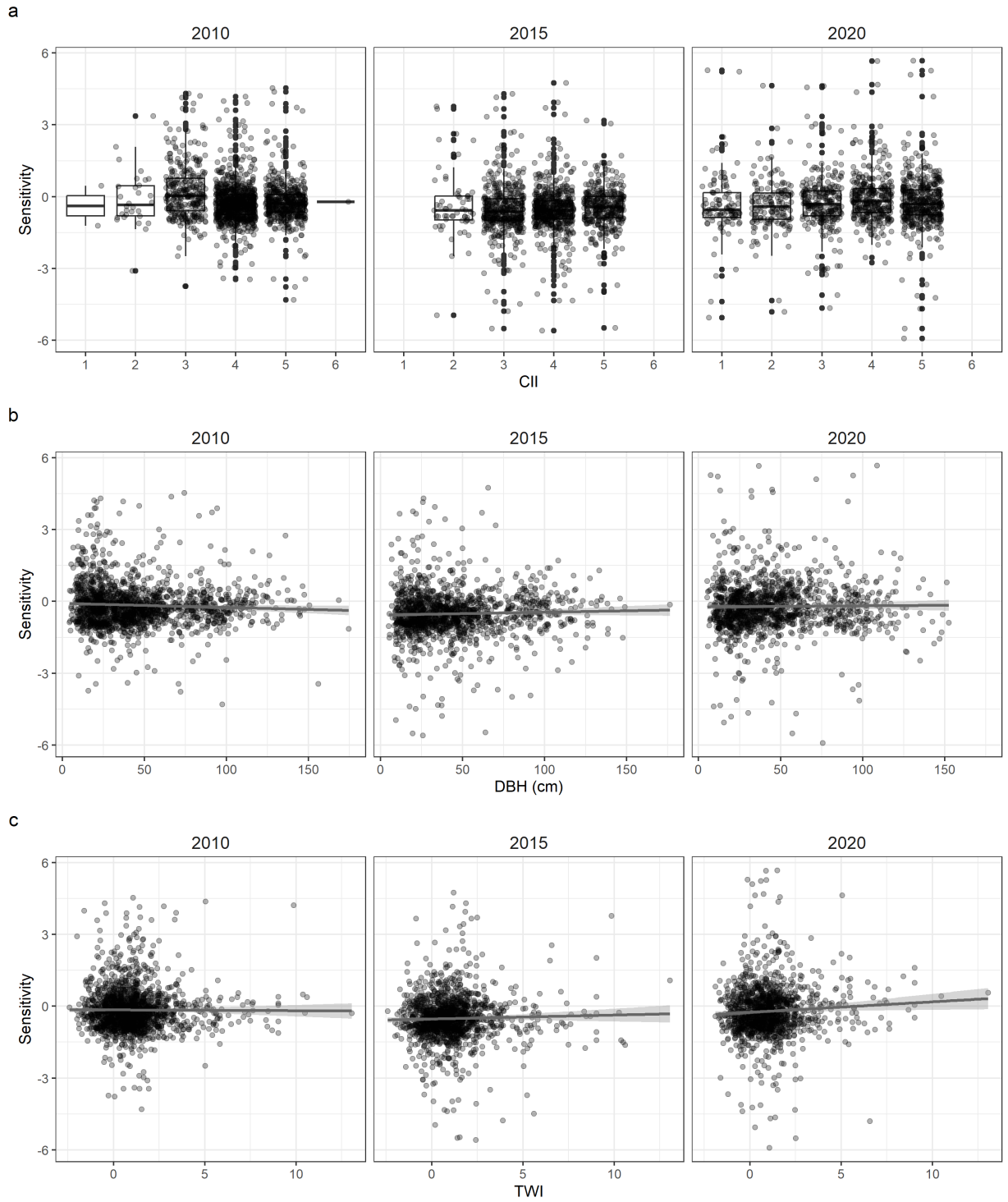


Figure S10: Distribution of raw sensitivity values across years and their relationship with DBH, CII and TWI. Lines are linear model fits.

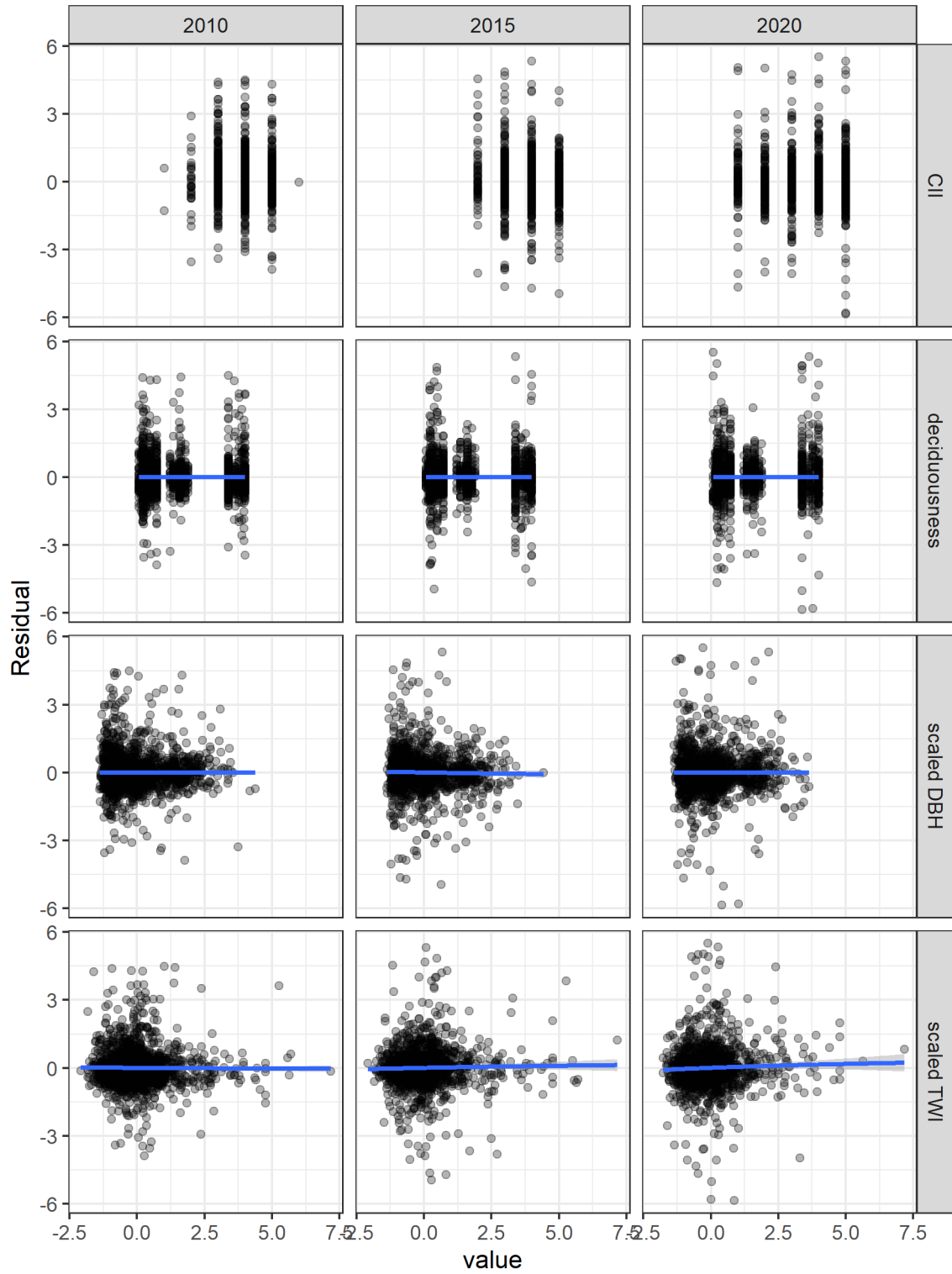


Figure S11: Distribution of residuals of species intercept models of sensitivity and their relationship with scaled DBH, TWI and CII and deciduousness. Species intercept model results are reported in main text.

Conditional dependencies

To analyse the influence of microenvironmental variables on growth sensitivity, we first created a Directed Acyclic Graph describing the relationships. To be able to test the DAG with the dataset, we used *dagitty* to derive the conditional dependencies that need to be tested, namely $CII \perp\!\!\!\perp TWI$ and $DBH \perp\!\!\!\perp TWI$.

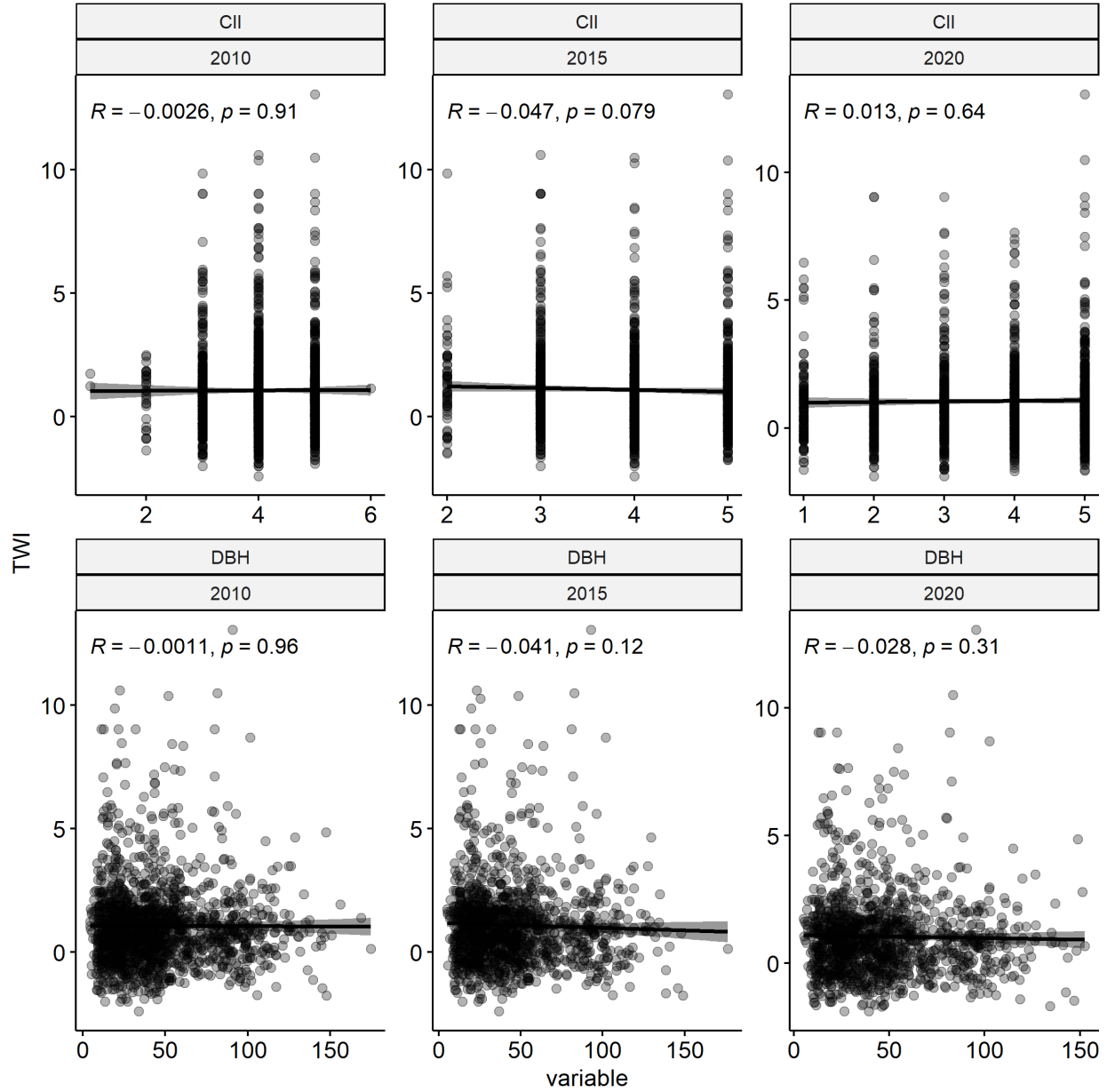


Figure S12: Testing correlations of variables across all individuals

There is low correlation between these two variable pairs across all individuals. We then tested conditional dependencies at the species level.

Most species (barring a few) had low correlation between these variables in our dataset, allowing us to proceed with analysis and interpretation.

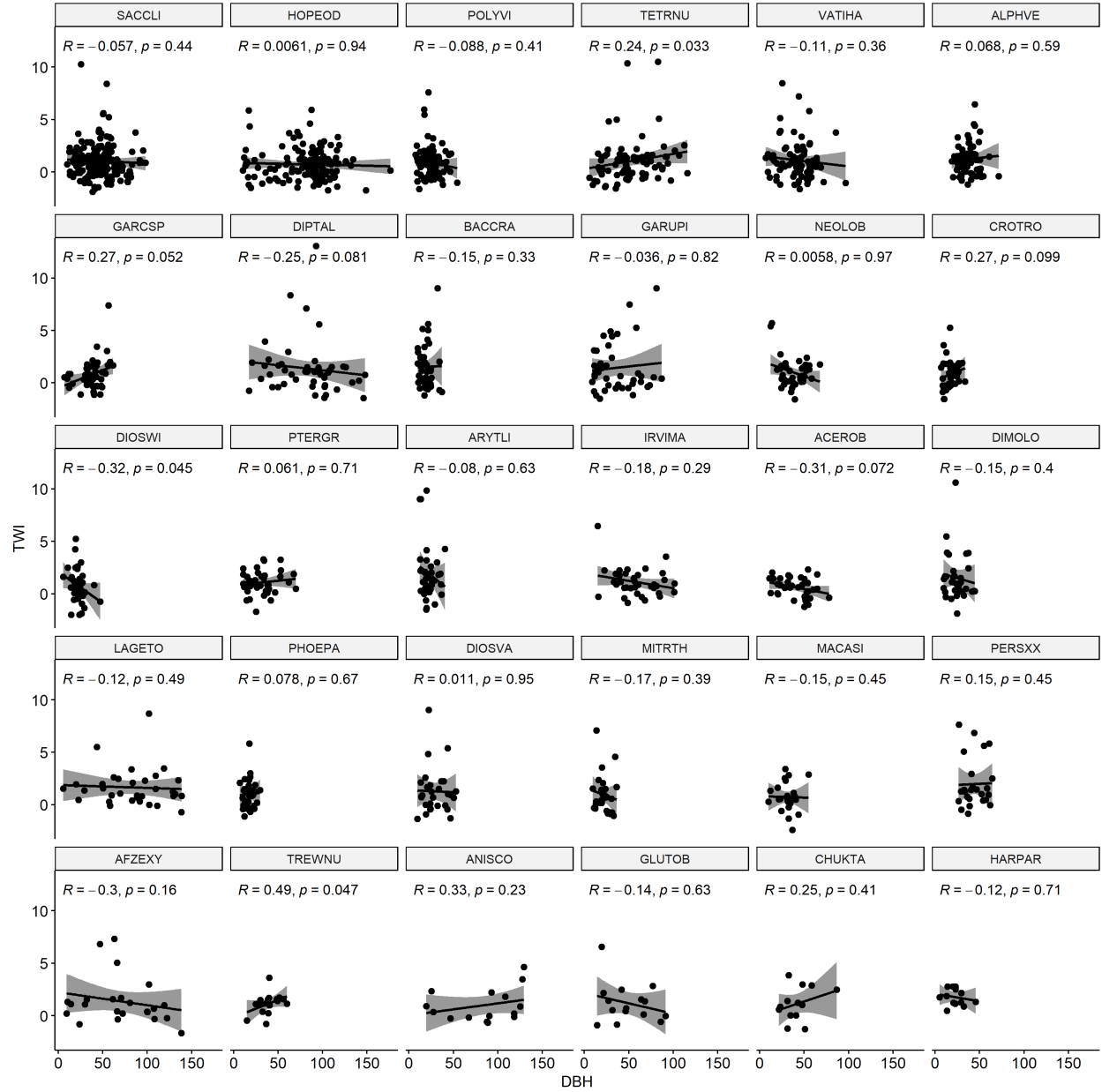


Figure S13: Testing correlations for DBH \perp TWI by species

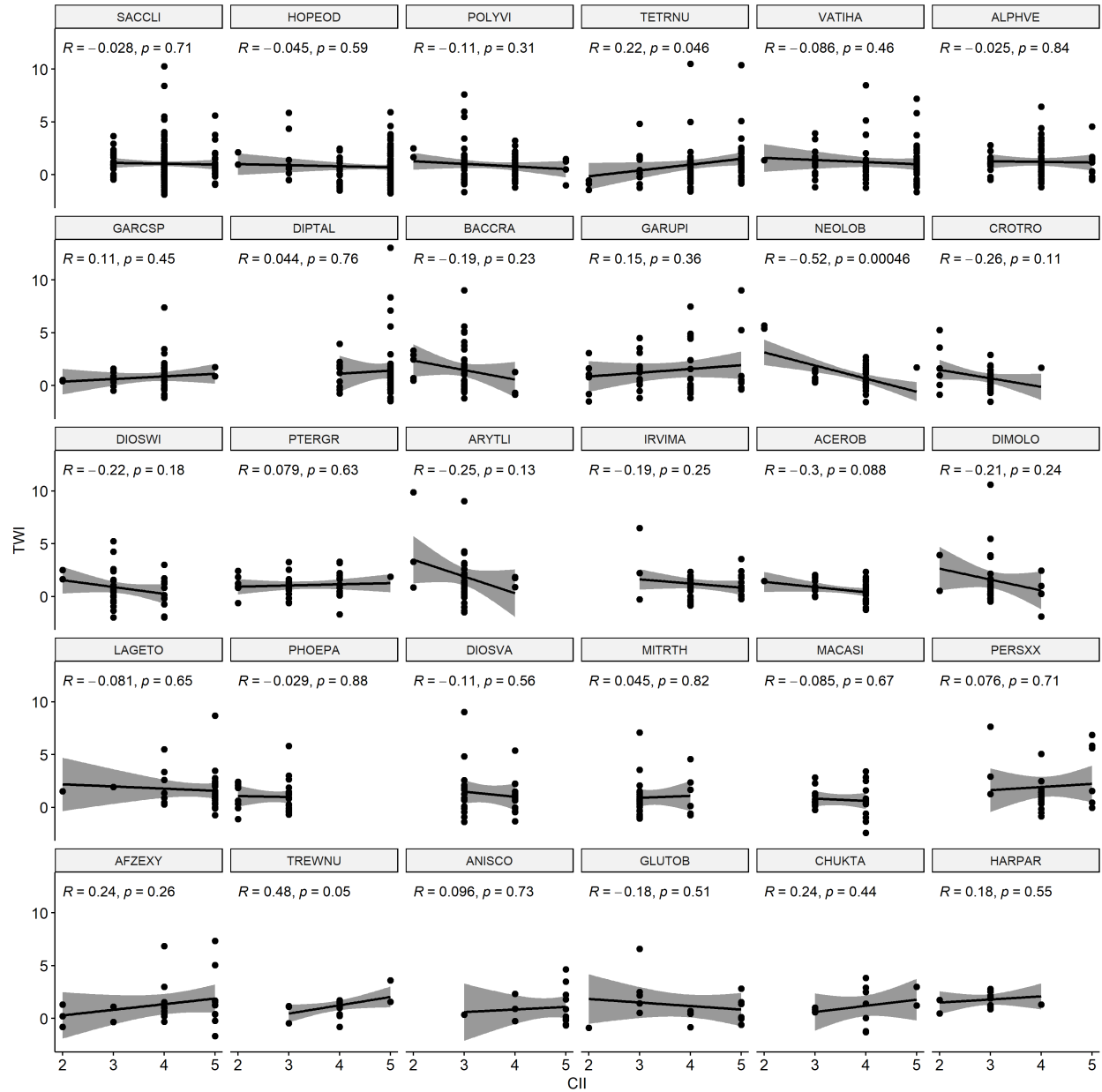


Figure S14: Testing correlations for $CII \perp TWI$ by species

Alternate models using Topographic Position Index

As an alternate measure of wetness to Topographic Wetness Index (TWI) that requires the total upslope area, we used Topographic Position Index (TPI), a localised convexity/concavity-based metric of water availability as a predictor. We calculated TPI using the package *spatialEco* (Evans & Murphy, 2023) using a circular buffer window of 1, 3, 5 and 7 pixels. Larger window sizes while providing a smoother surface on the plot, clip out larger portions of the plot margin where the window might bleed outside. We chose to use the 5-pixel version because of the balance between smoothness across the landscape and data loss.

TPI and TWI had better resolution in different parts of the wetness gradient, with TWI capturing larger resolution among wetter locations and TPI capturing larger resolution among drier locations. Interaction models of deciduousness with TPI showed qualitatively similar results with the TWI models across the three drought years.

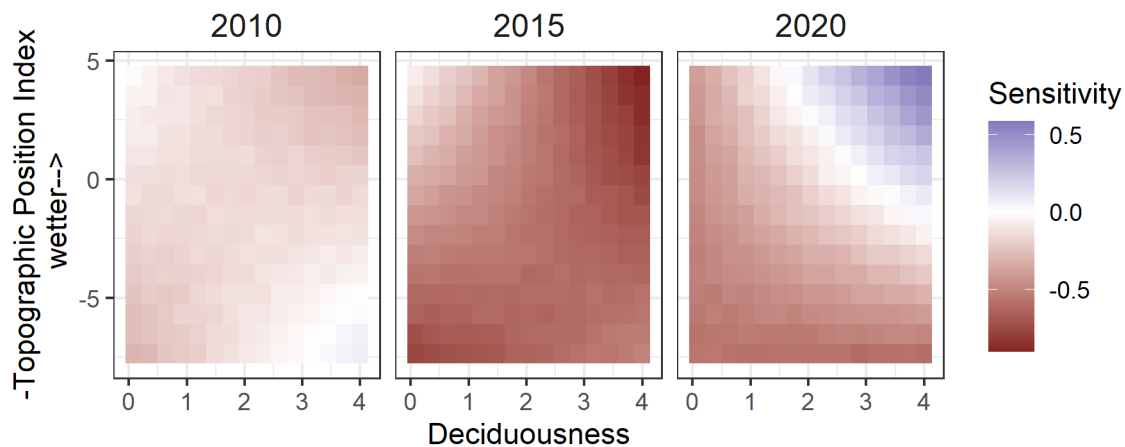


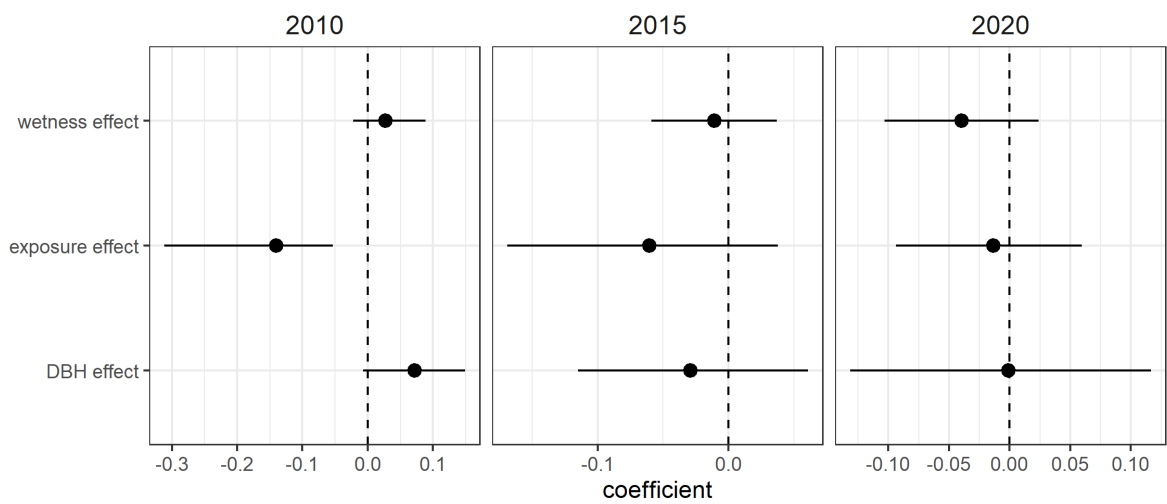
Figure S15: Correlation of modelled species sensitivities with Topographic Position Index

Similarly, models accounting for DBH and CII showed similar directional effects of wetness whether TWI or TPI was used. Please note that left to right represents wet to dry, given the way that TPI is calculated.

References

Evans JS, Murphy MA. 2023. *spatialEco*.

a



b

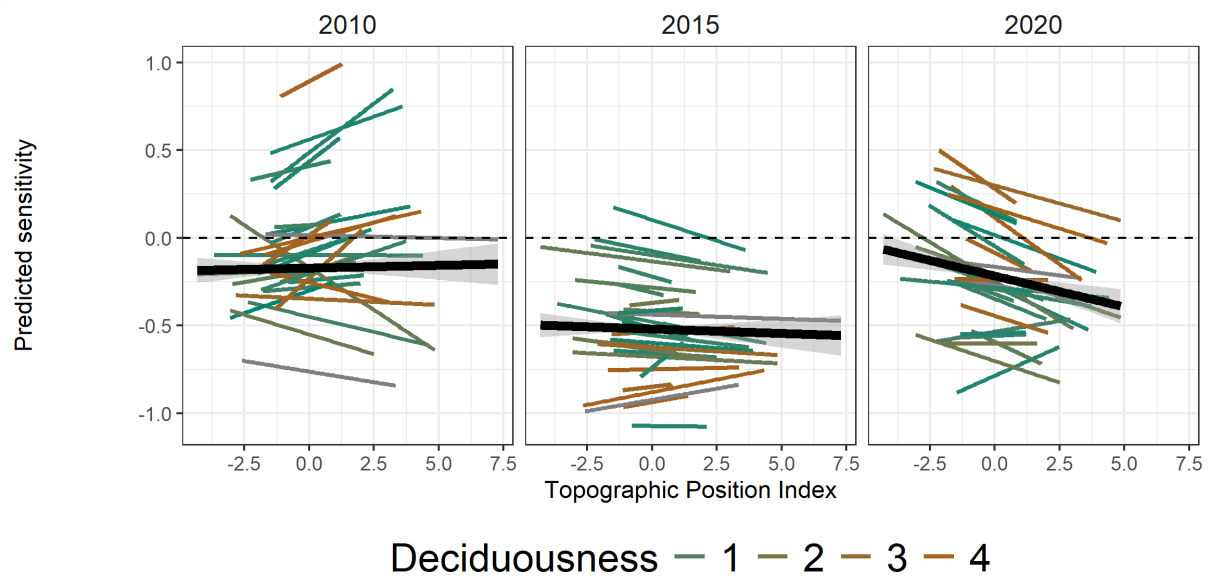


Figure S16: Model results from Bayesian causal model of sensitivity as a function of DBH, CII and TPI.